

# Reactions of Sulphate Radicals with Substituted Pyridines: A Structure–Reactivity Correlation Analysis

María L. Dell’Arciprete,<sup>[a]</sup> Carlos J. Cobos,<sup>[a]</sup> Jorge P. Furlong,<sup>[b]</sup> Daniel O. Mártire,<sup>[a]</sup> and Mónica C. Gonzalez\*<sup>[a]</sup>

*The kinetics of the oxidation of pyridine, 3-chloropyridine, 3-cyanopyridine, 3-methoxypyridine and 3-methylpyridine mediated by  $\text{SO}_4^{\cdot-}$  radicals are studied by flash photolysis of peroxodisulphate,  $\text{S}_2\text{O}_8^{2-}$ , at pH 2.5 and 9. The absolute rate constants for the reactions of both, the basic and acid forms of the pyridines, are determined and discussed in terms of the Hammett correlation. The monosubstituted pyridines react about 10 times faster*

*with sulphate radicals than their protonated forms, the pyridine ions. The organic intermediates are identified as the corresponding hydroxypyridine radical adducts and their absorption spectra compared with those estimated employing the time-dependent density functional theory with explicit account for bulk solvent effects. A reaction mechanism which accounts for the observed intermediates and the pyridinols formed as products is proposed.*

## Introduction

Pyridine and its derivatives are ubiquitous among naturally occurring products (i.e. nicotinamides and plant alkaloids) and xenobiotic chemicals such as insecticides, pesticides (i.e. nicotine, anabasin, cavadin, paraquat, imidachloprid, thiachloprid, diquat and pichloram), and industrial solvents. Pyridine is released to the environment mainly by industrial sources that manufacture and use it.

Abiotic oxidation of pyridine takes place in natural water resources, but with very low rates. A half-life of about 1.2 years is predicted from its hydroxyl radical-initiated decay with a bimolecular rate constant of  $1.8 \times 10^9 \text{ M}^{-1} \text{ s}^{-1}$  at 21 °C and pH 7<sup>[1]</sup> for a mean hydroxyl radical concentration of  $\sim 10^{-17} \text{ M}$ .<sup>[2]</sup> Pyridine reaction with other oxidizing species, such as the alkylperoxy radicals ( $\text{RO}_2^{\cdot}$ ), present in natural water is of no significance due to the low efficiency of these reactions, of  $\sim 0.67 \text{ M}^{-1} \text{ s}^{-1}$  at 50 °C.<sup>[2]</sup> On the other hand, there is a wide occurrence of pyridine degrading organisms,<sup>[3]</sup> complete pyridine biodegradation in unfiltered river water was reported to require between two to six months under aerobic conditions whereas between one to two months were required under anaerobic conditions.<sup>[4]</sup>

Investigations on pyridine electronic transitions and fragmentation usually involve pulse radiolysis studies.<sup>[5,6]</sup> The reaction pathways of abiotic pyridine degradation have not been thoroughly elucidated and scarce information is found in the literature concerning its depletion during the environmental remediation of waste sites by chemical procedures such as those employed by the advanced oxidation process (AOP) technologies<sup>[7]</sup> and in situ chemical oxidation (ISCO).<sup>[8,9]</sup> In particular, destruction of organic compounds included in water environments and soils by peroxodisulphate oxidation is gaining interest as an ISCO technology<sup>[8,9]</sup> because peroxodisulphate may be easily activated to yield the highly reactive sulphate radical ions ( $\text{SO}_4^{\cdot-}$ ).<sup>[10]</sup>

The study of the reactivity of pyridine substrates with  $\text{SO}_4^{\cdot-}$  radicals, and the characterization and reactivity of the organic radicals thus generated are of environmental and biological interest, since oxidation of pyridine derivatives is linked to many metabolic processes.<sup>[11,12]</sup> A correlation of the kinetic behavior of the different substituted pyridines with their chemical structure should bring some light to the role played by the pyridinic moieties in the radical-sensitized oxidation of biological molecules and insecticides.<sup>[13]</sup>

Photolysis of  $\text{S}_2\text{O}_8^{2-}$  with excitation wavelengths  $\lambda_{\text{exc}} < 300 \text{ nm}$ , Reaction (1), is a clean source of sulphate radical ions with high quantum yields, independent of pH in the range of 3–14.<sup>[14]</sup>



We report here a kinetic and mechanistic study on the reactions of  $\text{SO}_4^{\cdot-}$  with pyridine, 3-chloropyridine, 3-cyanopyridine, 3-methoxypyridine and 3-methylpyridine. In situ generation of  $\text{SO}_4^{\cdot-}$  is performed by flash photolysis of  $\text{S}_2\text{O}_8^{2-}$  aqueous solutions of  $\text{pH} \geq 2$ .

[a] M. L. Dell’Arciprete, Dr. C. J. Cobos, Dr. D. O. Mártire, Dr. M. C. Gonzalez  
Instituto de Investigaciones Físicoquímicas Teóricas y Aplicadas  
Facultad de Ciencias Exactas, Universidad Nacional de La Plata  
Casilla de Correo 16, Sucursal 4, (1900) La Plata (Argentina)  
Fax: (+54) 221-425-4642  
E-mail: gonzalez@inifta.unlp.edu.ar

[b] Dr. J. P. Furlong  
LADECOR, Departamento de Química, Facultad de Ciencias Exactas  
Universidad Nacional de La Plata (Argentina)

## Results

Reaction Rate Constants for  $\text{SO}_4^{\cdot-}$  Radicals with 3-Substituted Pyridines and Their Conjugated Acids

Laser or conventional flash photolysis of air-saturated  $\text{S}_2\text{O}_8^{2-}$  solutions of pH either 2.5 or 9, showed the formation of a transient species absorbing in the wavelength range from 300 to 600 nm, whose spectrum taken immediately after the flash of light, is in agreement with that reported in the literature for  $\text{SO}_4^{\cdot-}$ .<sup>[15]</sup> Photolysis of  $\text{S}_2\text{O}_8^{2-}$  in the presence of low concentrations ( $< 5 \times 10^{-5}$  M) of the substituted pyridines (XPy) showed absorption traces at detection wavelengths  $\lambda > 350$  nm, whose spectrum immediately after the flash of light also agrees with that for  $\text{SO}_4^{\cdot-}$  but with faster decay rates (see inset a of Figure 1). The decay of the  $\text{SO}_4^{\cdot-}$  absorbance,  $A$ , at a detection

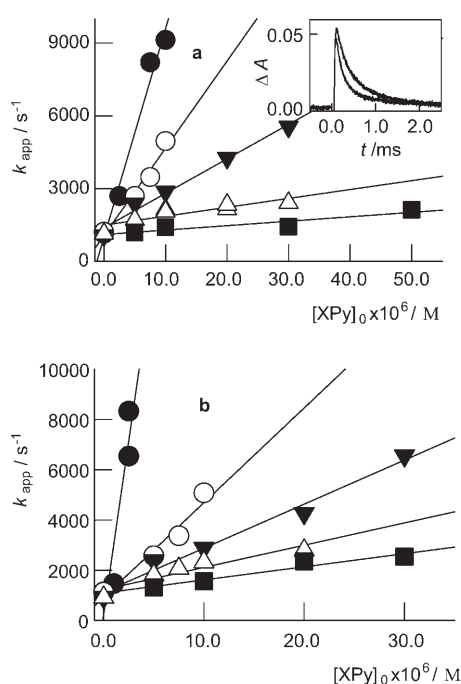


**Figure 1.** Apparent rate constant,  $k_{\text{app}}$ , versus  $[\text{XPy}]_0$  for 3-methoxypyridine (●), 3-methylpyridine (○), pyridine (▼), 3-chloropyridine (▽), and 3-cyanopyridine (■). Solutions of a) pH 2.5 and b) pH 9.0. Inset a: Absorbance change obtained at 450 nm for experiments with  $5.0 \times 10^{-3}$  M  $\text{S}_2\text{O}_8^{2-}$  aqueous solutions of pH 2.5 in the absence and presence of  $5 \times 10^{-6}$  M 3-methoxypyridine (upper and lower trace, respectively).

wavelength  $\lambda$  could be well fitted to Equation (2). The apparent rate constant,  $k_{\text{app}}$ , is independent of the wavelength  $\lambda$  and increases linearly with the analytical concentration of the substrate,  $[\text{XPy}]_0$ , as expected from Reaction (3) and shown in Figures 1 a and 1 b for experiments with solutions of pH 2.5 and 9, respectively. The small remnant absorbance [ $c(\lambda)$  in Eq. (2)] is associated with long-living species, mainly the organic radicals formed by Reaction (3).

$$A(\lambda) = a(\lambda) \cdot \exp(-k_{\text{app}} \cdot t) + c(\lambda) \quad (2)$$



The  $\text{p}K_{\text{a}}$  values of the substituted pyridines, shown in Table 1, strongly depend on the substituent.<sup>[16,17]</sup> Experiments with solutions of pH 9 yield information on the reaction of sulphate radicals with the substituted pyridines. However, experi-

**Table 1.**  $\text{p}K_{\text{a}}$  values,<sup>[16]</sup> Hammett parameters  $\sigma_{\text{p}}^+$  and  $k_{3,\text{XPy}}$  and  $k_{3,\text{XPyH}^+}$  for the different substituted pyridines at 293 K.

X in 	$\text{p}K_{\text{a}}$	$\sigma_{\text{p}}^+$	$k_{3,\text{XPy}} [\text{M}^{-1} \text{s}^{-1}]$	$k_{3,\text{XPyH}^+} [\text{M}^{-1} \text{s}^{-1}]$
			$I = 0.0016 \text{ M}$	$I = 0.005 \text{ M}$
CH <sub>3</sub> O-	4.88	-0.780	$(2.5 \pm 1) \times 10^9$	$(8.6 \pm 0.8) \times 10^8$
CH <sub>3</sub> -	5.68	-0.310	$(4.0 \pm 1) \times 10^8$	$(3.6 \pm 0.5) \times 10^8$
H-	5.17	0.000	$(1.8 \pm 0.2) \times 10^8$	$(1.4 \pm 0.8) \times 10^8$
Cl-	2.84	0.110	$(1.0 \pm 0.2) \times 10^8$	$(3.3 \pm 0.3) \times 10^7$
CN-	3.71	0.700	$(5.0 \pm 0.1) \times 10^7$	$(1.4 \pm 0.2) \times 10^7$

ments with solutions of pH 2.5 yield information on the reaction of sulphate radicals with the pyridinium ions with  $\text{X} = -\text{OCH}_3$ ,  $-\text{CH}_3$ ,  $-\text{H}$  and only partially for  $-\text{Cl}$  ( $\text{p}K_{\text{a}} = 2.84$ ) and  $-\text{CN}$  ( $\text{p}K_{\text{a}} = 3.71$ ). Lower pH solutions were avoided, since below pH 1 the conjugated acid ( $\text{HSO}_4$ ) of the sulphate radicals are formed. The absolute rate constants for the reactions of  $\text{SO}_4^{\cdot-}$  radicals with the substituted pyridines and pyridinium ions denoted as  $k_{3,\text{XPy}}$  and  $k_{3,\text{XPyH}^+}$ , respectively, are coincident with the slopes of the straight lines shown in Figures 1 a and 1 b, respectively, except for the values of 3-chloro and 3-cyano pyridinium ions. The absolute rate constants for these pyridinium ions were obtained from Equation (4) assuming fast acid-base equilibrium and taking the slopes  $s$  of the lines in Figure 1 a. Table 1 depicts all the calculated absolute rate constants.

$$k_{3,\text{XPyH}^+} = (s - k_{3,\text{XPy}}) \times \frac{K_{\text{a}}}{[\text{H}^+]} + s \quad (4)$$

The influence of the ionic strength on the rate constant of Reaction (3) for pyridine,  $k_{3,\text{XPy}}$ , and pyridinium ions,  $k_{3,\text{XPyH}^+}$ , was investigated. The rate constant  $k_{3,\text{Py}}$  does not depend, within the experimental error, on the ionic strength for  $I < 0.4$  M. On the other hand,  $k_{3,\text{PyH}^+}$  increases with decreasing ionic strength as shown in Equation (5), and expected for the aqueous phase reaction between two opposite charged ions with  $8.3 = \log k_{3,\text{PyH}^+}^0$  the logarithm of the reaction rate constant at zero ionic strength is:

$$\log k_{3,\text{PyH}^+} = 8.3 - 0.91 \times I^{1/2} \quad (5)$$

Both,  $k_{3,\text{XPy}}$  and  $k_{3,\text{XPyH}^+}$ , decrease with the electron-withdrawing ability of the substituent as expected from the electrophilicity of the sulphate radicals. Table 1 also shows the sigma Hammett parameters,  $\sigma_{\text{p}}^+$ .<sup>[18a]</sup> The substituent effect on these reactions can be quantitatively represented in a Hammett-type plot of the logarithm of the absolute rate constant versus  $\sigma_{\text{p}}^+$ ,<sup>[19]</sup> as shown in Figure 2. The plots using either  $\sigma_{\text{m}}^+$  or  $\sigma_{\text{o}}^+$ <sup>[18b]</sup> parameters (not shown) did not yield as good correla-

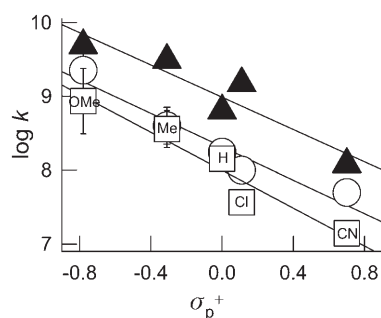


**Figure 2.** Logarithmic plots of  $k_3$  for XPy (○) and XPyH<sup>+</sup> (□) versus  $\sigma_p^+$ . The abbreviations H, Me, OMe, Cl and CN stand for the hydrogen, methyl, methoxy, chloro and cyano substituents, respectively. For comparison, the reported rate constants<sup>[20]</sup> for the reaction between the corresponding substituted benzenes and sulphate radicals are also shown (▲). The solid lines represent the linear correlation between  $\log k$  and  $\sigma_p^+$  ( $|r| = 0.93$  and  $0.917$  for the pyridines and the pyridinium ions respectively). Standard error bars are of the order of the symbol size, otherwise they are shown by brackets.

tions as those observed for  $\sigma_p^+$  values. The use of  $\sigma^+$  is a good option for the Hammett correlation in reactions where an electron-donating substituent interacts with a developing positive charge in the transition state, as seems to be the case for the reactions under study.<sup>[19]</sup>

The slopes  $\rho^+$  of the straight lines in Figure 2 are, within the experimental error, coincident ( $\rho^+ = -1.1 \pm 0.3$ ) despite that  $\text{SO}_4^{\cdot-}$  radical reactivity decreases with the different family of compounds as benzenes > pyridines > pyridinium ions.

### Organic Radicals Formed after the Reactions of $\text{SO}_4^{\cdot-}$ Radicals with 3-Substituted Pyridines and Pyridinium Ions

In order to characterize the organic radicals formed after Reaction (3), argon- or air-saturated  $5 \times 10^{-3} \text{ M}$   $\text{S}_2\text{O}_8^{2-}$  solutions of  $\text{pH} > 7$  with concentrations of substituted pyridines  $\geq 5 \times$

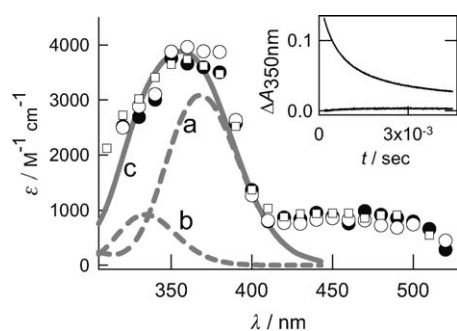


**Figure 3.** Absorption spectrum of the radicals observed in conventional flash-photolysis experiments with  $5 \times 10^{-3} \text{ M}$   $\text{S}_2\text{O}_8^{2-}$  and  $5 \times 10^{-5} \text{ M}$  3-methoxy-pyridine solutions of:  $\text{pH} 7$  with air (○) and argon (●) saturation. The dashed lines stand for the TD-DFT calculated spectrum for the 3-hydroxy-5-methoxy-pyridine (line a) and 2-hydroxy-5-methoxy-pyridine (line b) radical adducts. The solid line c stands for the  $a + 2.6 \times b$  combination. Inset: Transient and stable product (upper and lower trace, respectively) contribution to the absorption traces at  $350 \text{ nm}$  for experiments with the Ar-saturated solutions shown in the main figure. The fitting to a second order rate law is overlapped to the experimental curve.

$10^{-5} \text{ M}$  were irradiated either with a conventional flash lamp or a laser ( $\lambda_{\text{exc}} = 266 \text{ nm}$ ). Under these conditions, the  $\text{SO}_4^{\cdot-}$  lifetime is  $< 2 \mu\text{s}$ . The observed transients show absorption with maxima in the  $300\text{--}400 \text{ nm}$  range, depending on the nature of the substituent. The transient spectra are shown in Figures 3, 4, 5 (main panel and inset), and 6, for 3-methoxypyridine, 3-methylpyridine, pyridine, 3-chloropyridine, and 3-cyanopyridine, respectively.

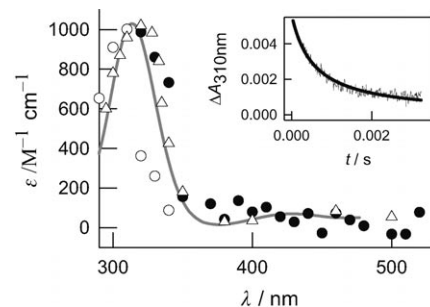


**Figure 4.** Absorption spectra of the radical observed in experiments with solutions at  $\text{pH} 9$ , (○):  $1 \times 10^{-3} \text{ M}$   $\text{S}_2\text{O}_8^{2-}$ ,  $1 \times 10^{-3} \text{ M}$  3-methylpyridine, saturated with argon (laser experiments), and (●):  $5 \times 10^{-3} \text{ M}$   $\text{S}_2\text{O}_8^{2-}$ ,  $1 \times 10^{-4} \text{ M}$  3-methylpyridine, saturated with air (conventional flash-photolysis experiments). (△): reported spectrum for the hydroxymethylpyridine radical adducts.<sup>[5]</sup> The solid line stands for that calculated for the 2-hydroxy-5-methylpyridine radical adduct by TD-DFT. Inset: Absorption trace obtained at  $310 \text{ nm}$  in the laser experiments of the main figure. The solid trace corresponds to the fitting to a second-order decay law.

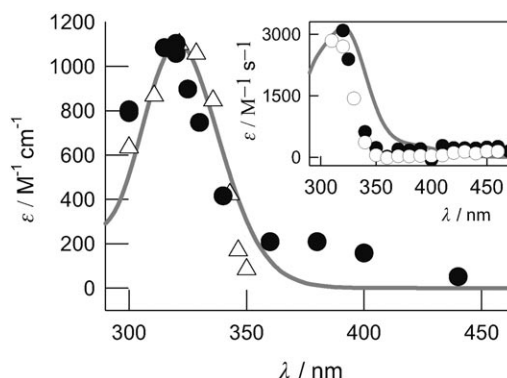


**Figure 5.** Absorption spectra of the radical observed in irradiation experiments with argon-saturated  $5 \times 10^{-3} \text{ M}$   $\text{S}_2\text{O}_8^{2-}$  solutions of  $\text{pH} > 7$  containing  $6 \times 10^{-4} \text{ M}$  of Py (●). Normalized reported spectrum of the hydroxypyridine radical adduct<sup>[5]</sup> (△). The solid line stands for the normalized spectrum of the 2-hydroxy-pyridine radical adduct calculated by TD-DFT. Inset: Absorption spectra of the transient observed in experiments with  $5 \times 10^{-3} \text{ M}$   $\text{S}_2\text{O}_8^{2-}$  solutions of  $\text{pH} 7$  containing  $5 \times 10^{-4} \text{ M}$  of 3-chloropyridine in air (○) and argon (●)-saturated solutions. The solid line stands for the normalized TD-DFT calculated spectrum of the 2-hydroxy-5-chloropyridine radical adduct.

For each substituted pyridine, several transient decay profiles were taken at different detection wavelengths within the range  $290\text{--}560 \text{ nm}$ . A bilinear regression analysis was applied to the absorbance matrix (see Experimental Section) to obtain information on the minimum number of species. For experiments with conventional flash photolysis, the bilinear analysis shows that the data obtained for the different pyridines may

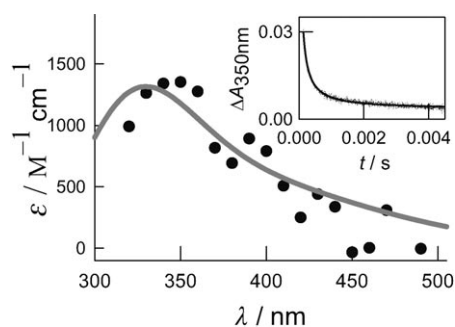


**Figure 6.** Absorption spectrum of the radical observed in irradiation experiments with air-saturated solutions of pH 7 containing  $5 \times 10^{-3}$  M  $S_2O_8^{2-}$  and  $5 \times 10^{-4}$  M 3-cyanopyridine (●). The solid line stands for the normalized TD-DFT calculated spectrum for the 2-hydroxy-5-cyanopyridine radical adduct. Inset: Time-resolved absorption at 350 nm for the experiments of the main figure, fitted to a second order rate law.

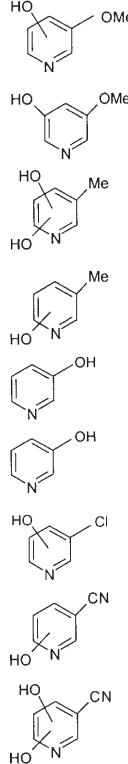
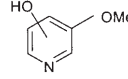
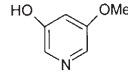
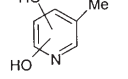
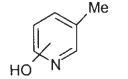
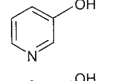
be described by two absorbing species: an organic transient already present 100  $\mu$ s after the flash of light, which decays to yield a stable product of lower absorbance, as depicted for 3-methoxypyridine in the inset of Figure 3.

The lower limit absorption coefficients for the organic transients, estimated from their maximum absorbance taking their concentration equal to the sulphate radical concentration reacting with the pyridine substrate, are shown in Table 2. The concentration of sulphate radicals is calculated from  $SO_4^{\cdot-}$  absorption traces obtained in experiments in the absence of pyridines, but otherwise identical conditions, taking  $\epsilon_{450nm} = 1600 \text{ M}^{-1} \text{ cm}^{-1}$ .<sup>[14]</sup>

For all the substituted pyridines, the decay of the organic radicals follow a second-order law, as shown in Figures 3 (inset), 4 (inset), and 6 (inset) for 3-methoxypyridine, 3-methylpyridine and 3-cyanopyridine, respectively. From the calculated absorption coefficients at the absorbance maxima, the recombination rate constants  $2 \times k_8$  for each organic transient is obtained and also shown in Table 2.

For 3-methylpyridine and pyridine, both, the transient spectra and decay rates are in agreement with those reported for the corresponding hydroxyl radical adducts<sup>[5]</sup> (see Figures 4 and 5) and may thus be assigned to these species. The lower limit absorption coefficients obtained herein are half the values reported by Solar et al.<sup>[5]</sup>

**Table 2.** Hydroxypyridine radical adduct decay rate constant ( $k_8$ ), wavelength of maximum absorption,  $\lambda_{max}$ , lower limit absorption coefficient at  $\lambda_{max}$  and observed products detected after irradiation of air-saturated aqueous solutions. The values of the mass to charge ratio of the molecular ions of the different analytes, detected by LC/MS, are also given.

X in 	$2 \times k_8$ [ $\text{M}^{-1} \text{s}^{-1}$ ]	$\lambda_{max}$ and in parentheses $\epsilon$ [ $\text{M}^{-1} \text{cm}^{-1}$ ]	Stable products [retention time (Rt), and principal mass peaks]	
$\text{CH}_3\text{O}-$	$(2.7 \pm 0.3) \times 10^8$ <sup>[a]</sup>	350 nm (3790) <sup>[a]</sup>	Rt = 1.4 min, $m/z = 148$ ( $125 + \text{Na}^+$ ), $126$ ( $125 + \text{H}^+$ ), $96$ ( $95 + \text{H}^+$ ). Rt = 1.3 min, $m/z = 148$ ( $125 + \text{Na}^+$ ), $126$ ( $125 + \text{H}^+$ ).	
$\text{CH}_3-$	$(3.2 \pm 1.5) \times 10^8$	320 nm (990, 2700) <sup>[5]</sup>	Rt = 1.5 min, $m/z = 110$ ( $109 + \text{H}^+$ ) Rt = 1.5 min, $m/z = 126$ ( $125 + \text{H}^+$ )	
H-	$(7.5 \pm 1) \times 10^8$	320 nm (1060, 2400 <sup>[21]</sup> , 4900 <sup>[5]</sup> )	Rt = 1.4 min, $m/z = 118$ ( $95 + \text{Na}^+$ ), and $96$ ( $95 + \text{H}^+$ )	
Cl-	$(1.0 \pm 0.2) \times 10^9$	320 nm (3400)	Rt = 1.4 min, $m/z = 118$ ( $95 + \text{Na}^+$ ), and $96$ ( $95 + \text{H}^+$ ) Rt = 1.1 min, $m/z = 130$ ( $129 + \text{H}^+$ )	
CN-	$(3.3 \pm 0.5) \times 10^9$	350 nm (1350)	Rt = 1.3 min, $m/z = 143$ ( $120 + \text{Na}^+$ ) Rt = 1.3 min, $m/z = 159$ ( $136 + \text{Na}^+$ )	

[a] Experimental value assuming one transient species. The calculated TD-DFT spectrum indicates it is the weight average due to the contribution of 2-hydroxy-5-methoxypyridine and 3-hydroxy-5-methoxy pyridine adducts.

Formation of transients of coincident absorption spectra and decay rates are observed in experiments with either argon- or air-saturated solutions, as shown in Figure 3 to Figure 5. To evaluate their reactivity towards molecular oxygen, the transient profiles were additionally fitted to a mixed first- and second-order law yielding acceptable residuals for first order rate constants up to  $1000 \text{ s}^{-1}$ . Substituted pyridinols are the main reaction products formed in experiments with air-saturated solutions, as shown in Table 2.

## Discussion

The previous results show that the reactions of 3-methylpyridine and pyridine with sulphate radicals lead to the formation of the respective hydroxypyridine radical adducts. From the good correlation between  $\log k_{3,\text{XPy}}$  and  $\log k_{3,\text{XPyH}^+}$  with the substituent constant,  $\sigma_p^+$ , shown in Figure 2, it may be expected that a similar reaction mechanism leading to the formation of substituted hydroxypyridine radical adducts applies for all the pyridines studied here. Because the Hammett-type plots yield the best correlation with the  $\sigma_p^+$  parameter, the sulphate radical addition to the pyridine ring in a position *para* to the substituent and *ortho* to the N group should be the preferred site of attack.

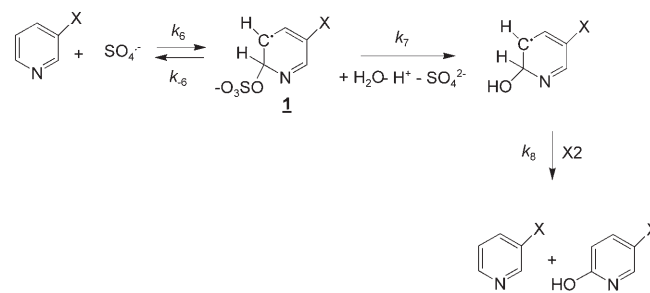
Hydroxyl adducts of pyridine and methylpyridines show acid–base dissociation constants which are approximately 0.5–0.6 pH units lower than the  $\text{p}K_a$  values of the parent pyridines.<sup>[5]</sup> The organic transient spectra reported here were obtained in solutions of  $\text{pH} > 7$  and therefore, the observed hydroxyl adducts are expected to be in their conjugated base form.

To prove the previous hypotheses the time-dependent density functional theory (TD-DFT) spectra of all the 2-hydroxy-5-substituted pyridine radical adducts were calculated and are shown for comparison in Figures 3 to 6. The excellent coincidence obtained between calculated and experimental transient spectra, except for the 3-methoxypyridine, indicates that the observed transients may be assigned to the corresponding 2-hydroxypyridine radical adducts. The transient spectrum observed for 3-methoxypyridine may be interpreted as due to the contribution of both, the 2-hydroxy-5-methoxypyridine and the 3-hydroxy-5-methoxypyridine radical adducts in a 2.6:1 ratio, in agreement with the formation of both, 2 or 4-hydroxy and 3-hydroxy-5-methoxypyridines as reaction product.

Hammett-type plots with slopes  $\rho^+ = -1.5 \pm 0.3$  (coincident with those in Figure 2) were suggested to indicate that  $\text{SO}_4^{\cdot-}$  radicals react by both, electron transfer and addition channels.<sup>[19]</sup> Formation of hydroxypyridine radical adducts after  $\text{SO}_4^{\cdot-}$  radical reaction with substituted pyridines may be explained by these reaction routes.

An electron transfer reaction from pyridine to  $\text{SO}_4^{\cdot-}$  radical anions is predicted to be thermodynamically unfeasible, since pyridine shows an oxidation peak potential in acetonitrile– $\text{Bu}_4\text{NPF}_6$  (0.1 M) of 2.46 V versus  $\text{Fc}/\text{Fc}^+$  [ $\text{Fc}$ : ferrocene,  $E^\circ(\text{Fc}/\text{Fc}^+ \text{ in water}) = +0.4 \text{ V}$  versus the normal hydrogen electrode (NHE)<sup>[22,23]</sup> and the sulphate radical reduction potential in

aqueous solutions is 2.43 V versus NHE.<sup>[24]</sup> However,  $\text{SO}_4^{\cdot-}$  radicals are known to react with high selectivity with substituted benzenes by an addition–elimination pathway yielding hydroxycyclohexadienyl radicals (HCHD).<sup>[25]</sup> Therefore,  $\text{SO}_4^{\cdot-}$  radical addition to the pyridine cycle and further elimination to yield hydroxypyridine radical adducts may be a probable reaction pathway, as shown in Scheme 1. A similar reaction scheme should apply for the protonated pyridine molecules.



**Scheme 1.** Mechanism of the reaction of sulphate radicals with 3-substituted pyridines.

The addition of sulphate radicals to substituted pyridines should involve the formation of sulphate adducts (1 in Scheme 1, not observed) followed by sulphate elimination and water addition yielding hydroxyl adducts. Pyridinol formation may take place after bimolecular hydroxypyridine adduct disproportionation, Reaction (8) in Scheme 1.

The good leaving group ability of sulphate ions may severely shorten the sulphate radical–pyridine adduct lifetime as also reported for the sulphate–benzene adducts<sup>[26]</sup> and therefore may not be observed with our experimental set-up. A kinetic analysis of the mechanism in Scheme 1 assuming steady-state conditions for the sulphate radical adducts 1, yields  $k_3 = \frac{k_5 \times k_7}{k_{-6} + k_7}$ . If the condition  $k_7 \gg k_{-6}$  applies, then  $k_3 = k_5$  as expected from the strong dependence observed for  $k_3$  with the nature of the substituent.

As already discussed,  $\text{SO}_4^{\cdot-}$  radical addition to the pyridine ring in a position *para* to the substituent and *ortho* to the N group might be the preferred site of attack. Moreover, sulphate radical reaction at the nitrogen position of 3-substituted pyridine molecules is not supported by our experimental results showing no pyridine N-oxide formation as a reaction product. The observed results are in agreement with reported data giving no definite indication on the occurrence of HO-attack at the nitrogen site<sup>[27,28]</sup> and with reported SCF MO calculations indicating that delocalization of the odd electron in the hydroxypyridine adducts favors their generation rather than hydroxyl addition to the N atom.<sup>[29]</sup>

Contrary to our observations, Dey et al.<sup>[28]</sup> suggested that an electron transfer was the preferred channel for the reaction of 3-aminopyridine with sulphate radicals. The one-electron oxidation potential of pyridine derivatives diminishes considerably with increasing electron donor ability of the substituents.<sup>[23]</sup> Since  $\text{NH}_2$  shows higher electron donor ability than those substituents studied here, the observed difference may be ex-

plained if the one electron reduction potential for the radical cation of 3-aminopyridine is  $< 2.4$  V versus NHE, and therefore the reaction is predicted to be thermodynamically feasible for that particular case.

H-abstraction from the methyl group of 3-methylpyridine may be a possible reaction channel competing with sulphate radical addition to the pyridine ring. However, our results do not give evidence for the formation of organic transients other than the hydroxymethylpyridine adduct, neither for the formation of pyridine products with an oxidized methyl group nor for products involving pyridine moieties bridged by methylene. Therefore, the H-abstraction reaction channel should be of no significance and the sulphate radical H-abstraction rate constant from methylpyridine is expected to be  $k_{\text{H-abs}} < 4 \times 10^8 \text{ M}^{-1} \text{ s}^{-1}$ . The H-abstraction from the methyl group was also observed to be of no significance for the reaction of HO· radicals with 3-methylpyridine.<sup>[5]</sup>

Formation of 3-hydroxypyridine as a reaction product of 3-chloropyridine may be explained by sulphate radical attack *ipso* to Cl, generation of the *ipso*-isomer of hydroxypyridine adduct, and further loss of HCl. A similar reaction path is reported for the sulphate radical reaction with chlorobenzene.<sup>[25]</sup>

Our experimental results show that formation and decay of 3-substituted hydroxypyridine radical adducts are not sensitive, within the experimental error, to the presence of molecular oxygen in air-saturated solutions. Therefore, oxidation of the pyridine moiety mainly rely on the disproportionation of the hydroxypyridine radical adducts to yield the corresponding pyridinols (see Scheme 1), in agreement with the nature of the products observed in experiments with air-saturated solutions. On the other hand, HCHD radicals, reversibly react with molecular oxygen to yield peroxy radicals, which after rearrangement to endoperoxides lead to the formation of open-chain oxidized products.<sup>[25]</sup> Therefore, substituted benzenes are expected to be more easily mineralized than pyridines substituted at a *meta* site of the N atom.

A value  $k_{\text{OX}} < 5 \times 10^6 \text{ M}^{-1} \text{ s}^{-1}$  is estimated for the rate constant of the reaction of the organic transients with O<sub>2</sub>. A rate constant  $k_{\text{OX}} = 7 \times 10^6 \text{ M}^{-1} \text{ s}^{-1}$  is reported for the reaction of O<sub>2</sub> with the hydroxyl adduct of 3-aminopyridine.<sup>[28]</sup> The reaction rates of O<sub>2</sub> with HCHD radicals increase with increasing electron donor ability of the substituents.<sup>[30]</sup> Assuming a similar behavior for the hydroxypyridine radical adducts, the reaction rate constant for the adducts studied here should be  $< 7 \times 10^6 \text{ M}^{-1} \text{ s}^{-1}$ , in agreement with the experimental observations. On the other hand,  $k_{\text{OX}} = 1 \times 10^8 \text{ M}^{-1} \text{ s}^{-1}$  is reported for the reaction of O<sub>2</sub> with the hydroxyl adduct of 2-aminopyridine,<sup>[28]</sup> thus indicating that the substitution site strongly influences the easiness of mineralization of the pyridine moiety.

## Experimental Section

3-Chloropyridine (99%), 3-methoxypyridine (97%), and 3-methylpyridine (99.5%) from Aldrich, 3-cyanopyridine (> 97%) from Fluka, pyridine (99.5%), potassium peroxodisulphate, NaOH, and HClO<sub>4</sub> from Merck, were used without further purification. Distilled water was passed through a Millipore system ( $> 18 \text{ } \Omega \text{ cm}^{-1}$ ,  $< 20$  ppb of

organic carbon). The pH value of the solutions was controlled by addition of either HClO<sub>4</sub> or NaOH as required and measured with a Consort pH meter model C832. Unless otherwise indicated the ionic strength, *I*, of the solutions was  $1.6 \times 10^{-2} \text{ M}$ . When required, the ionic strength was adjusted by addition of NaClO<sub>4</sub>.

Flash-photolysis experiments were carried out using either conventional flash lamps or a laser as irradiation source. The conventional apparatus was a Xenon Co. model 720C with modified optics and electronics.<sup>[31]</sup> Two collinear quartz Xenon high-intensity pulsed flash tubes, Xenon Corp. P/N 890–1128 [full width at half maximum (FWHM)  $\leq 20 \text{ } \mu\text{s}$ ], with a continuous spectral distribution ranging from 200 to 600 nm and maximum around 450 nm were used. The analysis source was a high-pressure mercury lamp (Osram HBO-100 W). The optical path length of the 1 cm internal diameter quartz sample cell was 10 cm. The monochromator collecting the analysis beam (Bausch & Lomb, high intensity) was directly coupled to a photomultiplier (RCA 1P28), whose output was fed into a digital oscilloscope (HP 54600B). Digital data were stored in a personal computer. The emission of the flash lamps was filtered with an aqueous solution highly concentrated in the corresponding aromatic compound in order to avoid photolysis of the substrate.

Laser flash-photolysis experiments were performed by excitation with the fourth harmonic of a Nd:YAG Litron laser (2 ns FWHM and 6 mJ per pulse at 266 nm). The analysis light from a 150 W Xe arc lamp, was passed through a monochromator (PTI 1695) and detected by a 1P28 PTM photomultiplier. Decays typically represented the average of 64 pulses and were taken by and stored in a 500 MHz Agilent Infiniium oscilloscope. The solutions had an absorbance of 0.3 at 266 nm. The photolysis of the substrates is negligible under the experimental conditions used. The temperature ( $20 \pm 3 \text{ } ^\circ\text{C}$ ) was measured inside the reactor cell with a calibrated Digital Celsius Pt-100  $\Omega$  thermometer. Freshly prepared solutions were used in order to avoid possible thermal reactions of peroxodisulphate with the substrates.

Reaction products were detected and identified by high-performance liquid chromatography–mass spectrometry (HPLC-MS) using a Agilent 1100 with diode array and electrospray ionisation (ESI) / single quadrupole detection equipped with a C18 Restek Pinnacle II column (250 mm  $\times$  2.1 mm internal diameter, particle size 5 micrometers) and using a mixture of acetonitrile/water 1/1 (v/v) as eluent at a 0.5 mL-per-minute constant flux. Detection limits were normally 1 ppm. The MS detector used a fragmentation potential of 70 eV in the positive mode with mass detection in the range from 50 to 200 amu. Samples for product detection were obtained from air-saturated solutions containing  $5 \times 10^{-3} \text{ M S}_2\text{O}_8^{2-}$  and  $2 \times 10^{-3} \text{ M}$  substituted pyridines irradiated with ten flashes of light. The organic substrates remaining in solution were extracted with a 1:1 CH<sub>2</sub>Cl<sub>2</sub>:MeOH mixture, the organic phase separated and evaporated until 1/3 of its volume and further diluted with a 1:1 acetonitrile:H<sub>2</sub>O mixture.

**Bilinear Regression Analysis:** For each experimental condition, several absorbance decay profiles at different detection wavelengths were taken. Absorbance is thus a function of wavelength and time. A bilinear regression analysis taking advantage of the linearity of the absorbance with both concentrations and absorption coefficients, was applied to the experimental absorption matrix in order to retrieve information on the minimum number of species and on their relative concentration profiles and absorption spectra.<sup>[32]</sup>

**Time-Dependent Density Functional Theory Calculations:** It has been shown that the time-dependent generalization of the density functional theory, TD-DFT, provides remarkable results in the calculation of the observed transition energies of the electronically ex-

cited states of a large number of molecules.<sup>[33]</sup> In particular, the theory gives a well-balanced description for conjugated molecules and open-shell systems such as excited states of radicals.<sup>[34]</sup> Herein, the recent O3LYP approach which combines the local exchange functional OPTX<sup>[35]</sup> with the correlation functional LYP<sup>[36]</sup> was employed. The OPTX was developed taking into account that exchange and left–right correlation are non-separable. To a more reliable comparison with the experiments, bulk solvent effects were evaluated employing the conductor-like polarizable continuum model, CPCM,<sup>[37]</sup> using for the water a dielectric constant of 78.39. It should be noted, that this is a suitable approach as long as no important specific interactions between the solute and solvent molecules are present. All calculations have been performed with the Gaussian 03 package.<sup>[38]</sup> The absorption spectra were computed following a two-step procedure. Firstly, the optimization of all structural parameters of each ground-state molecule (without symmetry constraints) was performed with the O3LYP/6–31G(d) functional *via* analytic gradient methods. In all the cases, real vibrational frequencies were obtained assuring that molecular structures correspond to energy minima. In the second step, the vertical electronic energies, the associated wavelengths of the band maxima,  $\lambda_{\text{max}}$ , and oscillator strengths were computed at the CPCM-O3LYP/6–311++G(d,p) level of theory. As a measure of the spin contamination, the expectation value of the  $\langle S^2 \rangle$  operator was not greater than 0.78, close to the exact value of 0.75 for doublet states.

The DF-DFT calculations do not account for vibrational broadening. Therefore, to compare with experimental results simulated spectra were obtained by representing each electronic transition with Gaussian shape functions centered at the calculated band maxima. The whole spectra are then obtained simply by summing over all derived transitions.

To explore the predictions for the absorption spectra of the intermediates species formed during the reactions of  $\text{SO}_4^{\cdot-}$  with the 3-substituted pyridines, the spectra of all reagents were first computed. To match the experimental maxima small shifts of the calculated  $\lambda_{\text{max}}$  were required. In addition, in the absence of a theoretical basis, to reproduce the shape of the spectra, different full width values,  $\sigma$ , at the 1/e height of the Gaussian bands were chosen. In this way, for the pyridine, 3-chloropyridine, 3-cyanopyridine, 3-methoxypyridine and 3-methylpyridine molecules values for  $\Delta\lambda_{\text{max}}$  of 27, –3, 7, 15 and 6 nm and for  $\sigma$  of 1600, 3200, 2400 and 1600  $\text{cm}^{-1}$  were required. The resulting absorption coefficients at the band peaks are between 5% (3-methoxypyridine) and 37% (3-methylpyridine) larger than the experimental ones. Taking into account the good agreement obtained, the spectra of the transient hydroxypyridines adducts were studied at the same DFT level of theory. For simplicity, a  $\sigma$  value of 1600  $\text{cm}^{-1}$  was employed for all intermediates.

## Acknowledgements

This research was supported by Agencia Nacional de Promoción Científica y Tecnológica, (PICT 06–14508 ANPCyT, Argentina) and Consejo Nacional de Investigaciones Científicas y Técnicas (CONICET). M.L.D. thanks ANPCyT for a graduate studentship. M.C.G. and C.J.C. are research members of CONICET. D.O.M. is a research member of Comisión de Investigaciones Científicas de la Provincia de Buenos Aires (CIC), Argentina. C.J.C. also thanks the Max Planck Institute for Biophysical Chemistry Göttingen (Karl Friedrich Bonhoeffer Institute) through the “Partner Group for Chloro-

fluorocarbons in the Atmosphere”. D.O.M. and M.C.G. thank the Deutsche Akademische Austauschdienst, DAAD, Alumni Program for an equipment grant.

**Keywords:** ab initio calculations · flash photolysis · photochemistry · radicals · reaction mechanisms

- [1] I. M. Dorfman, G. E. Adams, *Reactivity of the Hydroxyl Radical in Aqueous Solutions*, National Standard Reference Data System, Washington, DC, U.S. Department of Commerce, National Bureau of Standards, 1973.
- [2] T. Mill, D. G. Hendry, H. Richardson, *Chemical Oxidation Processes in Aquatic Systems: Oxidation of Cumene, Pyridine, and p-Cresol*, Report to Nation Science Foundation, Directorate for Applied Science and Research Applications, Washington, by Stanford Research Institute International, Physical Organic Chemistry Department, Menlo Park, CA. NSF/RA-790085. NTIS No. 298088, 1979.
- [3] C.-E. Kuo, S.-M. Liu, *Chemosph.* **1996**, *33*, 771–781.
- [4] R. A. Cassidy, W. J. Birge, J. A. Black, *Environ. Toxicol. Chem.* **1988**, *7*, 99–105.
- [5] S. Solar, K. Sehested, H. Holcman, *Radiat. Phys. Chem.* **1993**, *41*, 825–834.
- [6] J. A. LaVerne, I. Carmichael, M. S. Araos, *J. Phys. Chem. A* **2005**, *109*, 461–465.
- [7] H. Suty, C. De Traversay, M. Cost, *Water Sci. Technol.* **2004**, *49*, 227–233.
- [8] C. Liang, C. J. Bruell, M. C. Marley, K. L. Sperry, *Chemosph.* **2004**, *55*, 1225–1233.
- [9] D. Amarante, *Pollution Engineering*, **2000**, *32*, 40–42.
- [10] P. A. Block, R. A. Brown, D. Robinson, *Novel Activation Technologies for Sodium Persulphate In Situ Chemical Oxidation*, Preprint of the Proceedings of the Fourth International Conference on the Remediation of Chlorinated and Recalcitrant Compounds, **2004**.
- [11] J. Lamoureaux, A. Castonguay, *Carcinogenesis* **1997**, *18*, 1979–1984.
- [12] L. A. Damani, P. A. Crooks, M. S. Shaker, J. Caldwell, J. D’Souza, R. L. Smith, *Xenobiotica* **1982**, *12*, 527–534.
- [13] M. Abdollahi, A. Ranjbar, S. Shadnia, S. Nikfar, A. Rezaie, *Med. Sci. Monit.* **2004**, *10(6)*, 141–147.
- [14] W. J. McElroy, S. J. Waygood, *J. Chem. Soc., Faraday Trans.* **1990**, *86*, 2557–2564.
- [15] J. A. Rosso, P. Allegretti, D. O. Mártire and M. C. Gonzalez, *J. Chem. Soc., Perkin Trans. 2* **1999**, *2*, 205–210.
- [16] H. Reich, *J. Chem. Ed.* **2005**, *82*, 495; [http://research.chem.psu.edu/brpgrp/pKa\\_compilation.pdf](http://research.chem.psu.edu/brpgrp/pKa_compilation.pdf).
- [17] A. Albert, E. P. Serjeant, *The Determination of Ionization Constants*, 2nd Edition, Chapman and Hall, London, 1971.
- [18] a) J. March, *Effects of Structure on Reactivity*, in *Advanced Organic Chemistry, Reactions Mechanisms and Structure*, Wiley & Sons, New York, **1991**, Chap. 9; b) P. Segura, *J. Org. Chem.* **1985**, *50*, 1045–1053.
- [19] a) M. C. Gonzalez, D. O. Mártire, *Asian J. Spectrosc.*, **1999**, *3*, 125–128; b) D. O. Mártire, M. C. Gonzalez, *Progress in Reaction Kinetics and Mechanism*. **2001**, *26*, 201–218.
- [20] P. Neta, R. E. Huie, A. B. Ross, *J. Phys. Chem. Ref. Data* **1988**, *17*, 1027–1284.
- [21] B. Cercek, M. Ebert, *Trans. Faraday Soc.* **1967**, *63*, 1687–1698.
- [22] W. C. Barrette, H. W. Johnson Jr., D. T. Sawyer, *Anal. Chem.* **1984**, *56*, 1890–1898.
- [23] B. Reisttinen, V. D. Parker, *J. Am. Chem. Soc.* **1991**, *113*, 6954–6958.
- [24] P. Wardman, *J. Phys. Chem. Ref. Data* **1989**, *18*, 1637–1755.
- [25] J. A. Rosso, P. Caregnato, V. C. Mora, M. C. Gonzalez, D. O. Mártire, *Helvetica Chimica Acta* **2003**, *86*, 2509–2524.
- [26] S. Steenken, *One Electron Redox Reactions between Radicals and Organic Molecules. An Addition/Elimination (Inner-Sphere) Path: Topics in Current Chemistry*, Vol. 177, *Electron Transfer II*, Springer, Berlin **1996**, pp. 125–145.
- [27] S. Steenken, P. O’Neill, *J. Phys. Chem.* **1978**, *82*, 372–374.
- [28] G. R. Dey, D. B. Naik, P. Dwibedy, K. Kishore, *Radiat. Phys. Chem.* **2002**, *64*, 395–401.
- [29] M. C. Anthony, W. L. Waltz, P. G. Mezey, *Can. J. Chem.* **1982**, *60*, 813–819.

- [30] C. von Sonntag, H. P. Schuchmann in *The Chemistry of Free Radicals: Peroxyl Radicals in Aqueous Solutions*, (Ed. Z. B. Alfassi, Jhon), Wiley & Sons Ltd, Chichester, **1997**, pp. 173.
- [31] M. L. Alegre, M. Geronés, J. A. Rosso, S. G. Bertolotti, A. M. Braun, D. O. Mártire, M. C. Gonzalez, *J. Phys. Chem. A* **2000**, *104*, 3117–3125.
- [32] E. A. San Román M. C. Gonzalez, *J. Phys. Chem.* **1989**, *93*, 3532–3536.
- [33] K. B. Wiberg, R. E. Stratman, M. J. Frisch, *Chem. Phys. Lett.* **1998**, *297*, 60–64.
- [34] S. Hirata, M. Head-Gordon, *Chem. Phys. Lett.* **1999**, *302*, 375–382.
- [35] W.-M. Hoe, A. J. Cohen, N. J. Handy, *Chem. Phys. Lett.* **2001**, *341*, 319–328.
- [36] C. Lee, W. Wang, R. G. Parr, *Phys. Rev. B* **1988**, *37*, 785–789.
- [37] V. Barone, M. Cossi, *J. Phys. Chem. A* **1998**, *102*, 1995.
- [38] *Gaussian 03, Revision C.02*, M. J. Frisch, G. W. Trucks, H. B. Schlegel, G. E. Scuseria, M. A. Robb, J. R. Cheeseman, J. A. Montgomery, Jr., T. Vreven, K. N. Kudin, J. C. Burant, J. M. Millam, S. S. Iyengar, J. Tomasi, V. Barone, B. Mennucci, M. Cossi, G. Scalmani, N. Rega, G. A. Petersson, H. Nakatsuji, M. Hada, M. Ehara, K. Toyota, R. Fukuda, J. Hasegawa, M. Ishida, T. Nakajima, Y. Honda, O. Kitao, H. Nakai, M. Klene, X. Li, J. E. Knox, H. P. Hratchian, J. B. Cross, C. Adamo, J. Jaramillo, R. Gomperts, R. E. Stratmann, O. Yazyev, A. J. Austin, R. Cammi, C. Pomelli, J. W. Ochterski, P. Y. Ayala, K. Morokuma, G. A. Voth, P. Salvador, J. J. Dannenberg, V. G. Zakrzewski, S. Dapprich, A. D. Daniels, M. C. Strain, O. Farkas, D. K. Malick, A. D. Rabuck, K. Raghavachari, J. B. Foresman, J. V. Ortiz, Q. Cui, A. G. Baboul, S. Clifford, J. Cioslowski, B. B. Stefanov, G. Liu, A. Liashenko, P. Piskorz, I. Komaromi, R. L. Martin, D. J. Fox, T. Keith, M. A. Al-Laham, C. Y. Peng, A. Nanayakkara, M. Challacombe, P. M. W. Gill, B. Johnson, W. Chen, M. W. Wong, C. Gonzalez and J. A. Pople, Gaussian Inc., Pittsburgh, PA, **2004**.

---

Received: July 6, 2007

Revised: September 8, 2007

Published online on October 24, 2007